Recycling of nutrient transporters from yeast endosomes is regulated by ubiquitinated Ist1

Kamilla ME. Laidlaw[1], Grant Calder[2], Chris MacDonald[1*]

[1] *York Biomedical Research Institute and Department of Biology, University of York, York, UK*
[2] *Imaging and Cytometry Laboratory, Bioscience Technology Facility, Department of Biology, University of York, UK*
[*] *Correspondence: Email: chris.macdonald@york.ac.uk Tel: +44 (0) 1904 328 609*

ABSTRACT

Trafficking of cell surface membrane proteins through a dynamic network of endomembrane compartments ensures correct cellular function. Upon internalisation, many surface proteins are either degraded or recycled back to the plasma membrane. Although these pathways control many biological processes, the precise regulatory features and division of labour between interconnected pathways is unclear. Using the budding yeast *Saccharomyces cerevisiae,* our work suggests retrograde recycling via the *trans*-Golgi Network (TGN) of cargoes like yeast synaptobrevins (Snc1 / Snc2), that rely on cargo ubiquitination, is distinct from endosomal trafficking of nutrient transporters. We provide evidence that nutrient transporters internalise to, and upon deubiquitination recycle from, endosomes marked by Vps4 and Ist1. A genetic screen for this recycling pathway previously implicated the ESCRT-III associated factor Ist1, suggesting Ist1 functionally defines yeast recycling endosomes. We demonstrate Ist1 ubiquitination affects its endosomal recruitment and ability to promote recycling. Finally, we reveal the ubiquitin-binding adaptor Npl4 and the essential ATPase Cdc48 are also involved in recycling. Our work suggests features of endosomal recycling are evolutionarily conserved.

INTRODUCTION

The plasma membrane (PM) hosts a wide variety of functionally diverse membrane proteins that are regulated by membrane trafficking pathways. Surface proteins can be downregulated through endocytosis and trafficking to the lysosome (vacuole in yeast), for example in response to stimuli or stress[1–3]. Endocytosed surface cargoes that retain a ubiquitination signal are targeted through the multivesicular body (MVB) pathway, packaged into intraluminal vesicles (ILVs) and then delivered to the vacuole for degradation[4,5]. Ubiquitinated cargoes are recognised by the Endosomal Sorting Complex Required for Transport (ESCRT) complexes, with ESCRT-0 and ESCRT-I abundant in ubiquitin binding domains[6]. ESCRT-III subunits are recruited to the endosomal / MVB membrane, where they polymerise and drive formation of vesicles budding into the lumen of [7–9]. Filaments created through polymerisation of Snf7, modulated by other ESCRTs and the Vps4 ATPase, drive membrane deformation[10–14]. Nutrient transporters in yeast are useful reporters for endosomal trafficking, such as the amino acid transporters Mup1 and Fur4, as their ubiquitination and ESCRT-dependent trafficking to the vacuole can be triggered by addition of substrate[15–17]. The E3-ligase Rsp5, which is competitively recruited through substrate specific adaptors[18,19], is largely responsible for ubiquitination of such cargoes, which predominantly traffic to the vacuole.

Surface activity of internalised PM proteins is also regulated by recycling routes back to the PM[20]. Recycling in yeast appears less complex than mammalian cells but the division of labour between certain pathways and even organisation of the endosomal system, is not fully understood[21–23]. The best characterised recycling route in yeast is the retrograde pathway, used by the yeast homologues of synaptobrevin, Snc1 and Snc2, that are required for transport vesicle fusion with the plasma membrane[24]. Localisation of Snc1 is polarised with concentration to the bud-tips of emerging daughter cells and the shmoo protrusions induced

upon response to mating factor; this polarisation relies on post-endocytic recycling[25]. Recycling of Snc1 via the *trans*-Golgi Network (TGN) is thought to rely on multiple pathways involving different machinery, such as retromer, Snx4-Atg20[26–28] and other factors, such as phospholipid flippases, Rcy1, and Ypt31/32[29–33]. One curious observation is that the retrograde recycling of Snc1 also requires its ubiquitination to facilitate interaction with endosomally localised COPI[34]. However, deubiquitination of other cargoes, like nutrient transporters that are typically sorted to the vacuole upon ubiquitination, appears to have the opposite effect. Directing catalytic activity of deubiquitinating enzymes (DUb) cancels cargo degradation and triggers recycling by default, which has been achieved by direct DUb-fusion to cargo or indirectly via Rsp5 and ESCRT proteins[35–37]. Most convincingly, dimerization of endosomally localised cargo results in nutrient transporter return to the PM[38].

To characterise this pathway, a genetic screen using a DUb fused version of the receptor Ste3 was performed to reveal 89 factors that are required for this recycling[39], most of which were validated with additional assays, including the growth benefits of efficiently recycling the tryptophan permease Tat2 in low tryptophan media[40] and tracking the recycling of the lipid dye FM4-64[41]. Null mutants of retrograde machinery like retromer, Snx4/41/42 and Ere1/2[27,42,43] were not identified by the screen and recycle FM4-64 at similar rates to wild-type cells[39]. Furthermore, cells harbouring a mutant allele of *SEC7* with abrogated transit through the Golgi also exhibit efficient DUb-triggered recycling. Intriguingly, some endosomal machinery that Snc1 relies on was shown to be required for recycling (Rcy1, Cdc50-Drs2, Ypt31/32), suggesting some, but not all, Snc1 trafficking pathways[44] might share compartments / machinery. Collectively, these data suggest the recycling of DUb-fused cargoes is largely distinct from retrograde recycling of Snc1, but there is likely overlap between routes. The Ste3-DUb-fusion screen did not identify any ESCRT nulls as defective for recycling, indeed recycling is more efficient in some ESCRT nulls[36,45], however, the ESCRT-like protein Ist1 was shown as required for recycling.

Ist1 shares structural homology with other ESCRT-III subunits and contributes to the efficiency of MVB sorting[14,46–50]. Ist1 interacts with other ESCRT-III subunits and Vps4, the AAA-ATPase required for MVB sorting and disassembly of ESCRT polymers[51–55]. Ist1 regulation of Vps4 is complex, as even *in vitro* Ist1 can stimulate and inhibit Vps4 activity and control depends on other ESCRT-III subunits[56]. Therefore, despite great strides in our understanding of ILV formation by ESCRT-III filaments and Vps4[11,12,14,57] our understanding of the role(s) of Ist1 in the endosomal assemblage *in vivo* is incomplete. Furthermore, high levels of Ist1 inhibit MVB sorting and diverse cargoes are sorted more efficiently to the vacuole in *ist1*Δ cells[58]. Therefore, in addition to the negative regulation of Vps4, it may be that Ist1 also promotes an opposite acting recycling pathway to the PM. In support of this idea, *in vivo* and *in vitro* studies show that unlike ESCRT-III polymers, which drive luminal vesicle formation, Ist1 polymerisation exerts the opposite effect on endosomal membranes to generate tubulation of cytosolic protrusions[59]. Physiologically this can be best rationalised by Ist1 promoting the recycling pathway by creation / fission of recycling tubules that return material back to the PM in collaboration with the ATPase spastin[60,61].

In this study we present evidence that Snc1/ Snc2 mainly recycle via a trafficking route to the TGN that is distinct from the pathway used by nutrient transporters for methionine (Mup1) and uracil (Fur4), which rapidly internalise to compartments marked by Vps4 and Ist1. Endosomal trafficking of Mup1/Fur4 proceeds to the vacuole in the presence of substrate. However, upon removal of the substrate-induced degradation signal, Mup1 recycles back to the PM with little evidence of traversing the TGN. This recycling pathway driven by deubiquitination relies on the ESCRT-III associated protein Ist1, and we provide initial evidence that Ist1 ubiquitination and Cdc48-Npl4 is required for efficient recycling. We present a hypothetical model that these observations are connected and that functionally distinct yeast endosomes might share machinery.

RESULTS

Differential cargo recycling routes in yeast

The v-SNARE Snc1 is a well-established retrograde cargo that internalises and recycles via the Golgi back to the plasma membrane (PM) through multiple pathways[26,44]. Snc1 ubiquitination is required for recycling[34] and the fusion of a deubiquitinating enzyme (DUb) catalytic domain is sufficient to block recycling of GFP-tagged Snc1 and the paralogue Snc2 (**Figure 1A**). In contrast, substrate induced ubiquitination of the Mup1 (methionine) or Fur4 (uracil) permeases does not promote recycling and instead drives endocytosis and vacuolar degradation[15,16,62,63]. The fusion of either Mup1 or Fur4 to a DUb domain antagonises vacuolar sorting[35], resulting in an increase in surface localisation, even in the presence of substrate (**Figure 1B**). Retrograde recycling of Snc1 / Snc2 via the TGN is required for its polarised PM distribution[25–28], with GFP tagged Snc1 / Snc2 concentrated in budding daughter cells (**Figure 1C, 1D**).

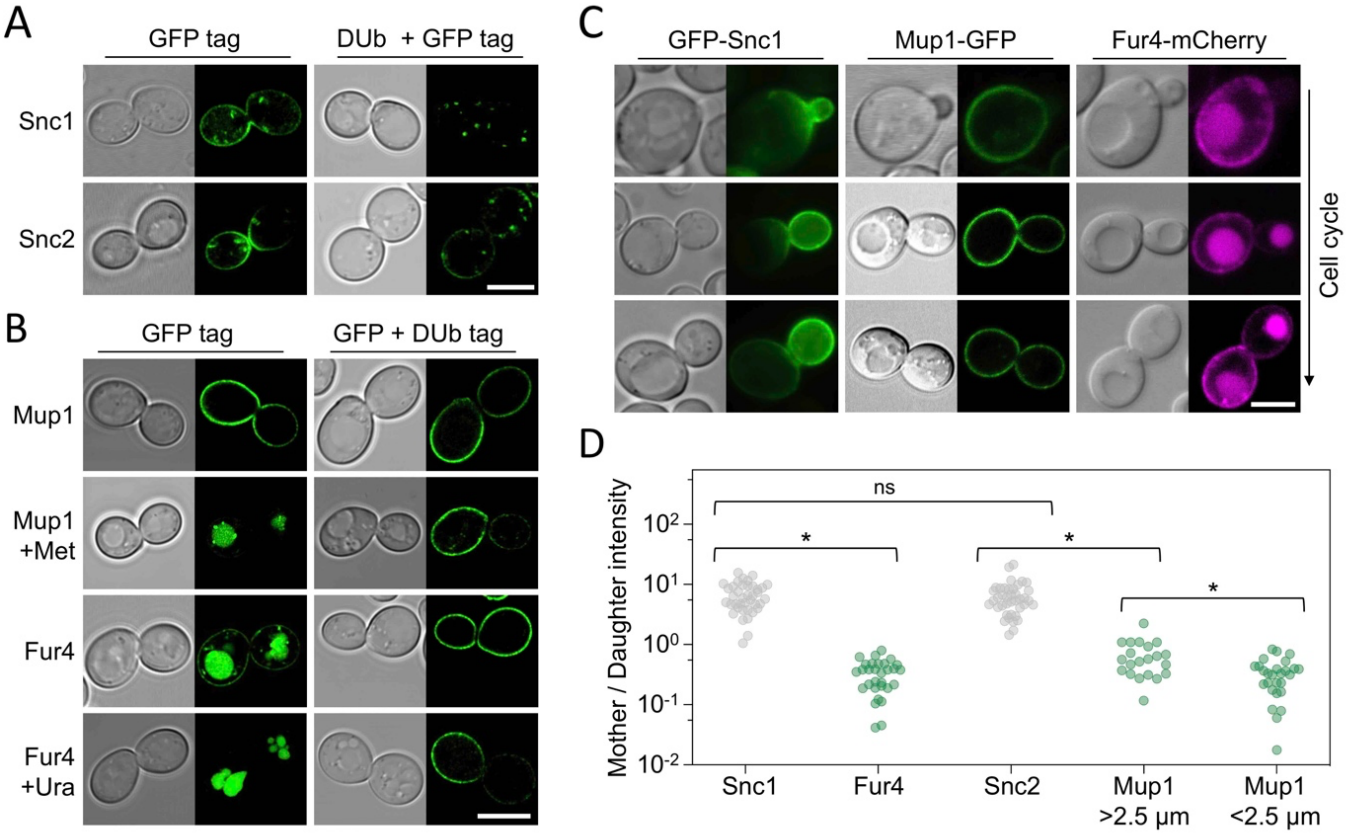

Figure 1: Differential trafficking features of recycling cargoes. ***A)*** Wild-type cells expressing versions of Snc1 and Snc2 N-terminally tagged with either GFP or a fusion of GFP with the catalytic domain of deubiquitinating enzyme UL36 (DUb + GFP) expressed from the *CUP1* promoter were grown to mid-log phase in the presence of 100 µM copper chloride and imaged by Airyscan confocal microscopy. ***B)*** Wild-type cells expressing Mup1 and Fur4 from their endogenous promoters and fused to C-terminal GFP or GFP-DUb tags were imaged by Airyscan. Where indicated, 20 µg/ml methionine (+Met) and 40 µg/ml uracil (+Ura) was added to media for 1-hour prior to imaging. ***C)*** Wild-type cells grown to mid-log phase and expressing fluorescently labelled Snc1, Mup1 and Fur4 were imaged, with example micrographs for different stages of the cell cycle shown. ***D)*** Quantification of PM fluorescence of indicated cargoes (GFP-Snc1, GFP-Snc2, Fur4-nMG, Mup1-GFP) in daughter cells relative to mother. Error bars show standard deviation from > 21 cells per cargo * denotes p value < 0.002 from unpaired *t*-test. Scale bar, 5 µm

Unlike Snc1 / Snc2, fluorescently tagged Mup1 and Fur4 concentrate in the mother cell during budding (**Figure 1C, 1D, S1A-C**), with polarisation maintained through the cell cycle for Fur4 but being chiefly in small cells (<2.5 µm diameter) for Mup1. Although cargo-specific trafficking regulation might explain these mother-daughter differences, taken with the opposing effects of enforced deubiquitination, we hypothesize that PM recycling of nutrient transporters relies on a distinct mechanism than Snc1 / Snc2. As expected, intracellular signal from retrograde cargoes Snc1 / Snc2 colocalises with the TGN marker Sec7-mCherry, with very little overlap with the endosomal marker Vps4-mCherry (**Figure 2A, 2B S2A-C**). The majority of intracellular signal is from recycling Snc1, and not first-pass molecules transiting the Golgi, as a mutant version of Snc1 with defective internalization[26] (Snc1^{PM}) exhibits very little intracellular signal; any intracellular GFP-Snc1^{PM} colocalises with Sec7-mCherry (**Figure 2C**). Furthermore, DUb-GFP-Snc1 / Snc2 fusions, which do not recycle efficiently, accumulate in Sec7-marked TGN compartments (**Figure 2D, 2E**). In contrast, intracellular Mup1-GFP, triggered by substrate or nutrient starvation[37,38] primarily internalise to Vps4-mCherry, and not TGN, compartments (**Figure 2F - 2G**). Similarly, Fur4-mNG that has significant intracellular signal irrespective of substrate presence colocalises with Vps4 endosomes (**Figure 2H - 2I**).

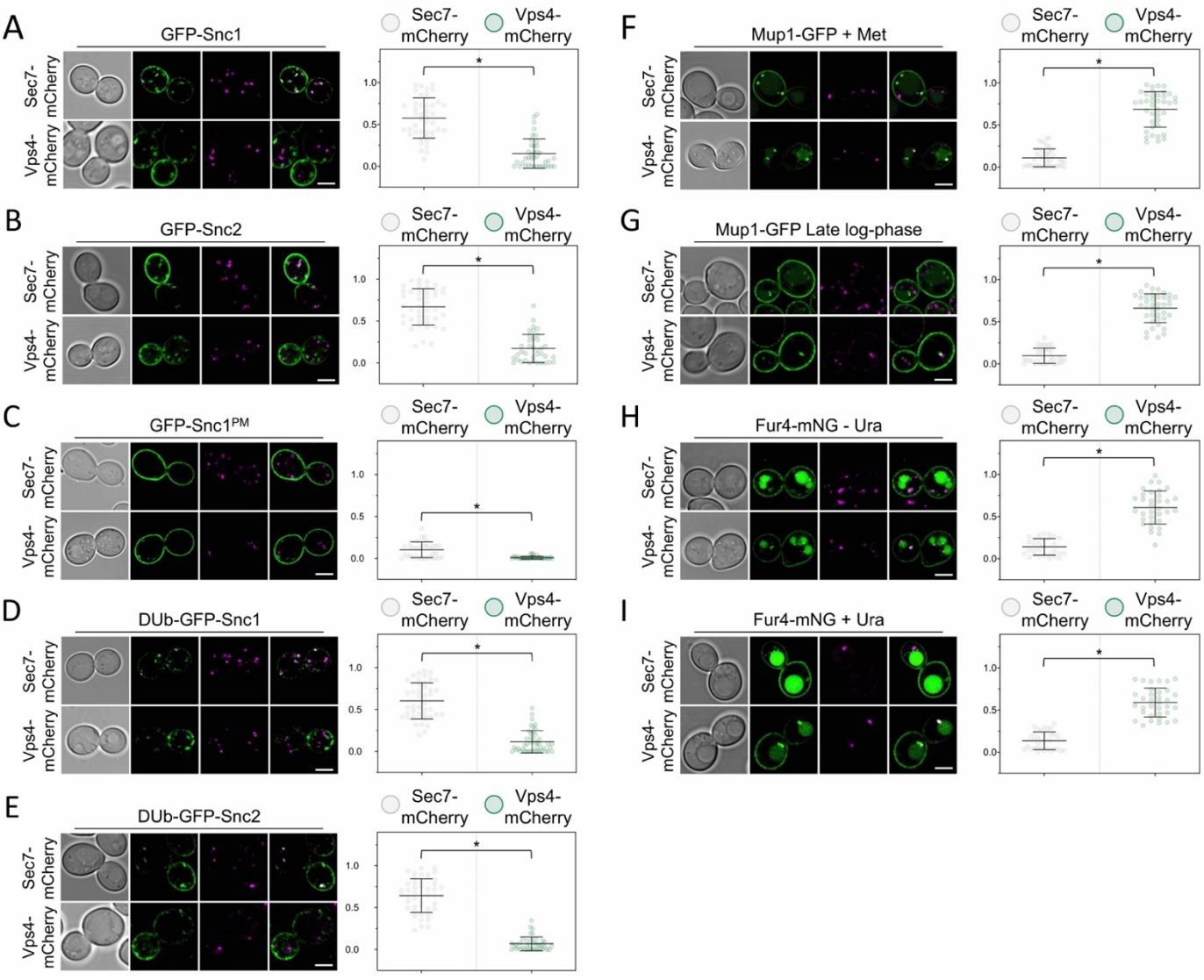

Figure 2: Differential recycling of internalised cargo to Sec7 and Vps4 -marked compartments. ***A-I)*** Indicated cargoes were imaged by Airyscan microscopy in cells expressing genomically tagged versions of either Sec7-mCherry (upper micrographs) or Vps4-mCherry (lower micrographs), with associated jitter plots of Mander's overlap coefficients (n ≥ 30) shown in grey and green, respectively (right). * denotes p value < 0.0001 from unpaired *t*-test. ***A-E)*** GFP or DUb-GFP tagged versions of Snc1, Snc2 and an endocytic mutant (Snc1^{PM}) were expressed from the *CUP1* promoter with 100 µM copper chloride at imaged at log-phase. ***F-G)*** Mup1-GFP was internalised by addition of 20 µg/ml methionine (+Met) or growth to OD_{600} = ~2.0 (late log-phase). ***H-I)*** Fur4-mNG was imaged in minimal media lacking uracil (-Ura) or 15 minutes after addition of 40 µg/ml uracil (+Ura). Scale bar, 5 µm.

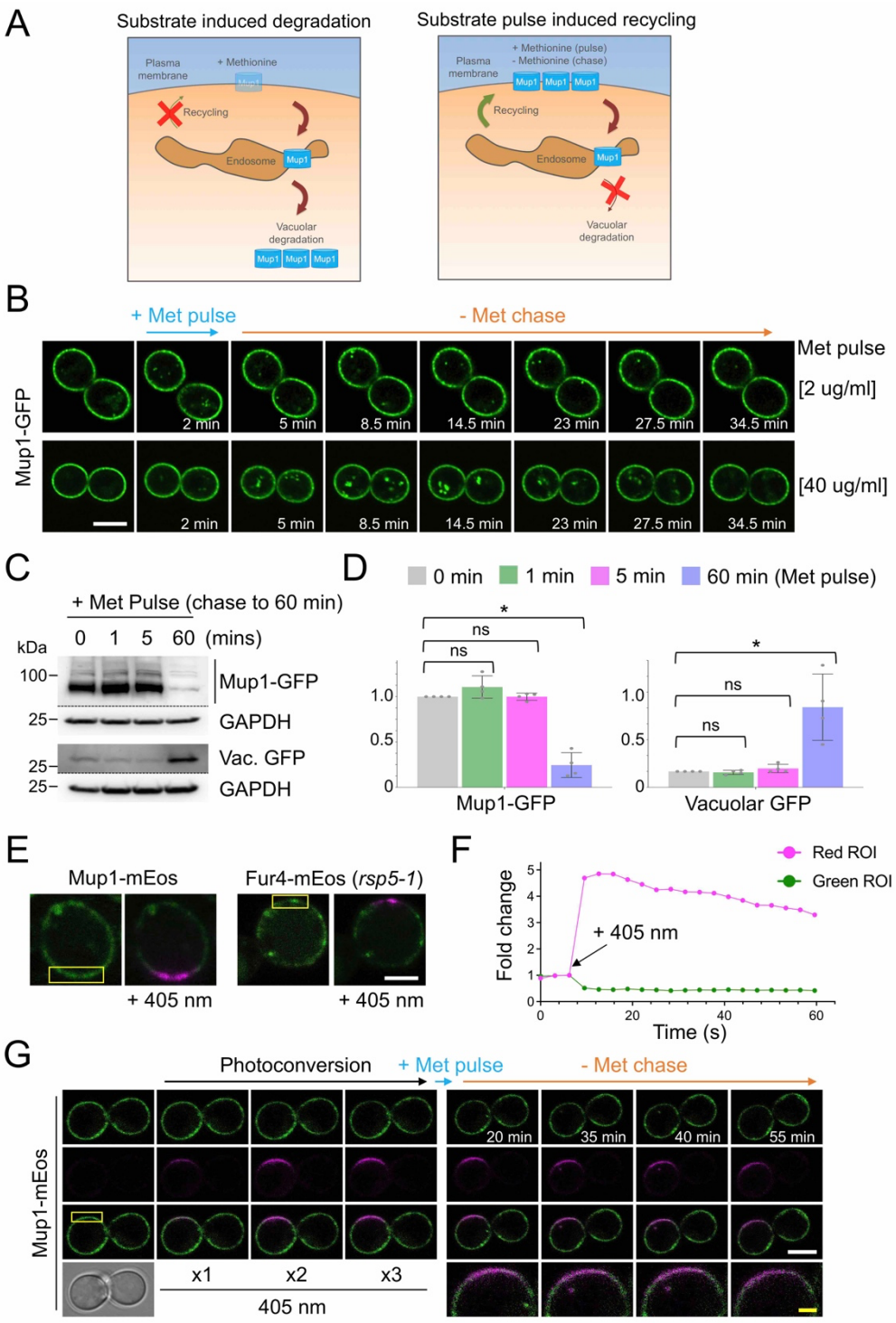

Figure 3: Substrate induced cell surface recycling. ***A)*** Schematic representation of substrate induced degradation (left) and recycling (right) of Mup1 triggered by modulation of extracellular methionine. ***B)*** Wild-type cells expressing Mup1-GFP were adhered to ConA coated coverslip plates from OD_{600} = ~0.1 cultures followed by time-lapse Airyscan microscopy before and after 2-minute methionine (2 µg/ml, upper and 40 µg/ml, lower) pulse-chase incubations were performed with microfluidics. ***C)*** Mid-log phase cells expressing Mup1-GFP were incubated with 20 µg/ml methionine for 0, 1, 5 and 60 mins followed by 3x washes and growth in SC-Met up to 60-minutes total incubation before lysates generated and used for immunoblot with anti-GFP antibodies and anti-GAPDH as a loading control. ***D)*** Quantification of average intensity of Mup1-GFP (left) and vacuolar processed GFP (right) from methionine pulse-chase experiments from (***C***). n = 4 biological replicates, error bars show standard deviation from unpaired *t*-test * represents p > = 0.01. ***E)*** Wild-type cells expressing Mup1-mEos (left) and Fur4-mEos (right) were grown to mid-log phase and processed for microscopy. Yellow box indicates regions exposed to 405 nm laser at 0.5%, with shown post conversion micrographs indicated (right). ***F)*** Line graph showing mEOS fluorescence intensity fold change over time before and after 405nm laser photo-conversion. ***G)*** Time lapse microscopy of wild-type cells expressing Mup1-mEOS, adhered to ConA coverslip plates from early log phase cultures, including 3 pulses of photoconversion with 0.1% 405 nm laser followed by substrate induced recycling stimulated with 30 second 2 µg/ml methionine pulse-chase protocol. Scale bar represents 5 µm (white), 1 µm (yellow).

.

Nutrient transporters recycle from early endosomes

Although enforced deubiquitination of nutrient transporters promotes PM recycling, observing recycling of unmodified nutrient transporters is hampered by their proclivity for vacuolar sorting[35–38]. To overcome this, we optimised microfluidic exchange with continuous imaging to perform a substrate pulse, followed by washes and a substrate-free chase to allow internalised cargo to recycle naturally (**Figure 3A**). Mup1-GFP was used for these experiments as it exhibits steady state localisation at the PM, and we found high (40 µg/ml) and low (2 µg/ml) levels of methionine triggered accumulation of intracellular puncta, with high doses giving brighter, more obvious signal (**Figure 3B**). The pulse-chase protocol resulted in accumulation of intracellular Mup1-GFP for 0-15 minutes followed by clearance of most signal after an additional 15 minutes, regardless of methionine pulse concentration. To avoid concerns about photobleaching or substrate induced degradation, biochemical analysis was used to show that methionine pulse periods of 1 or 5 minutes, followed by substrate free chase up to 60 minutes resulted in no increase in vacuolar delivery of internalised Mup1-GFP (**Figure 3C, 3D**). All subsequent substrate induced experiments were performed with <1 minute methionine pulses. Next, to confirm intracellular nutrient transporter signal emanated from the surface, we optimised photoconversion of surface localised Mup1-mEos and Fur4-mEos (**Figure 3E**, **3F, S3A-C**). By coupling cargo photoconversion to microfluidic induced recycling and time-lapse microscopy, we demonstrate signal of intracellular Mup1 from the PM, which subsequently dissipates with similar kinetics to Mup1-GFP recycling (**Figure 3G, Movie S1**). We then followed the trafficking itinerary of internalised and recycled Mup1-GFP using 4D confocal Airyscan microscopy optimised for rapid acquisitions. Methionine induced internalisation was tracked with fast acquisitions (4 - 10 second intervals) to show substantial intracellular accumulations that colocalise with Vps4-mCherry, and not Sec7-mCherry within the first few minutes (**Figure 4A**, **4B, Movie S2, S3**). Additionally, Mup1-GFP recycling experiments were imaged over longer periods (using 30 - 60 second time intervals) to show Mup1 primarily traverses Vps4 endosomes, bypassing Sec7-mCherry compartments (**Figure 4C**, **4D, Movie S4, S5**). An additional series of Mup1-GFP recycling experiments were quantified for colocalisation with either Vps4-mCherry and Sec7-mCherry at different time-points to show the bulk of Mup1 internalises and recycles from Vps4 endosomes (**Figure 4E**). We did note that that Mup1-GFP colocalises to a small but significant degree with Sec7-mCherry over time-lapse experiments, almost all overlap was TGN compartments adjacent with the PM, which might be explained by rapid trafficking to TGN compartments in the vicinity of the PM, TGN-PM contact sites, or due to an imaging artifact (**Figure S4**).

Ist1 is required for cargo recycling

Vps4, the ATPase involved in ESCRT-mediated ILV formation, marks a large and relatively static endosome reminiscent of Vps8 compartments[21] in addition to a population of peripheral mobile compartments[11]. The ESCRT-associated factor Ist1 colocalises with Vps4 in both populations, in addition to potentially distinct endosomes (**Figure 4F, Movie S6**). These compartments show no colocalization with Sec7-marked TGN compartments, suggesting recycling occurs from Ist1 endosomes. Ist1 was the only recycling factor from a blind genetic screen[39] that also interacts with Vps4 (**Figure 4G**), suggesting Ist1 might functionally define this population of recycling endosomes. We integrated the Ste3-GFP-DUb recycling reporter to confirm recycling defects of *ist1*Δ and *rcy1*Δ cells, in addition to quantifying their capacity for recycling Tat2 via growth on low Tryptophan and FM4-64 efflux (**Figure 4I - 4J**).

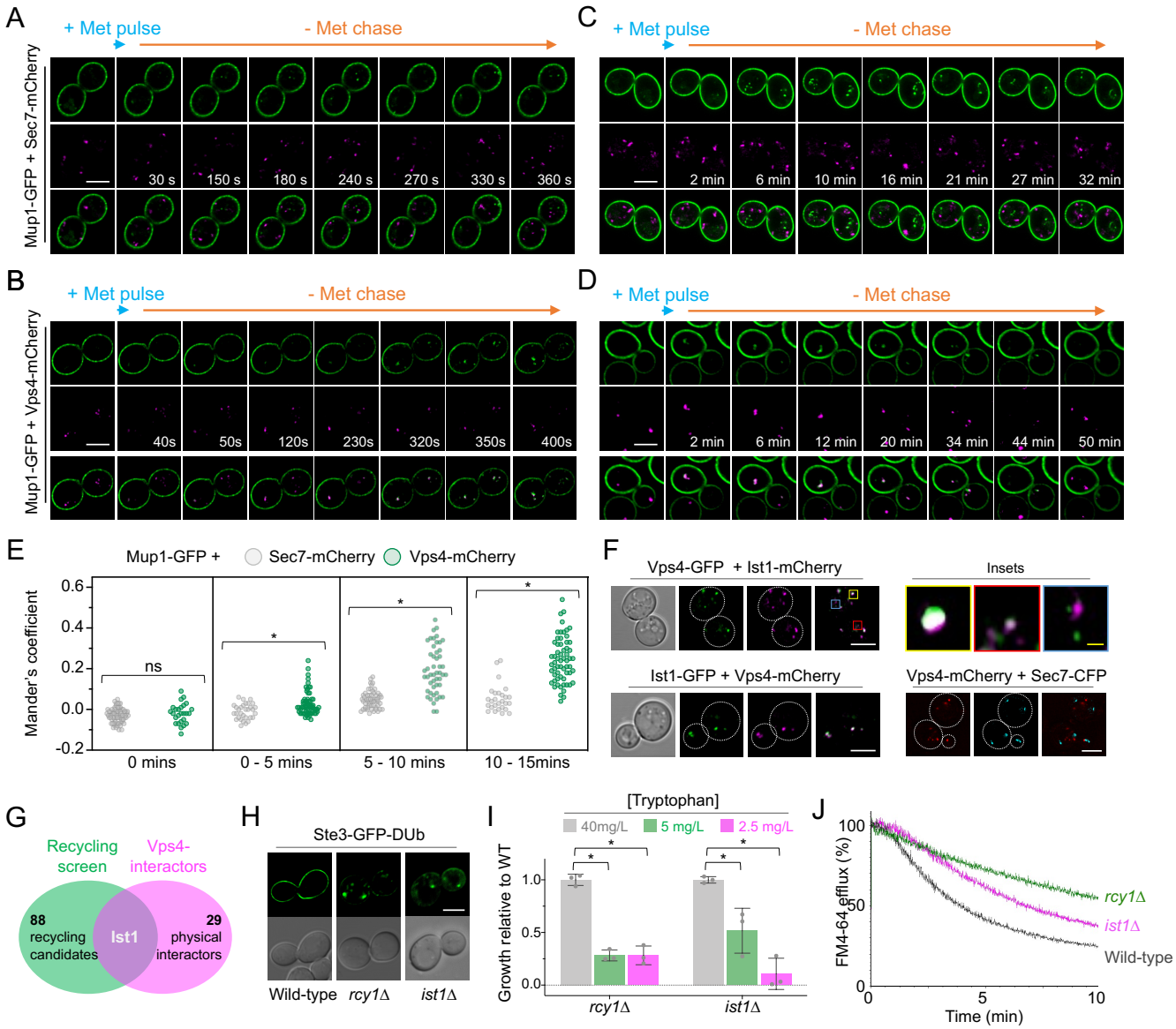

Figure 4: Mup1-GFP recycling occurs from a Vps4-Ist1 endosome

A-B) 4D Airyscan microscopy of wild type cells co-expressing Mup1-GFP and Sec7-mCherry ***(A)*** and Vps4-mCherry ***(B)*** following a 30 second 20 µg/ml methionine pulse and subsequent SC-Met chase period over short (left) and long (right) imaging intervals. ***C)*** Jitter plot quantification of Pearson's correlation coefficients of intercellular Mup1-GFP signal to either Sec7-mCherry (grey) or Vps4-mCherry (green) signal at indicated times of 20 µg/ml methionine pulse-chase protocol. n = >27 cells, * represents $p < 0.002$ from unpaired *t*-test. ***D)*** Wild type cells co-expressing fluorescently labelled versions of Ist1, Vps4 and Sec7 were imaged by Airyscan microscopy. Blue inset denotes areas of minimal co-localisation and yellow inset denotes areas of maximal co-localisation. ***E)*** Venn diagram showing 89 factors identified as required for recycling and known physical interactors of Vps4. ***F)*** Stably integrated Ste3-GFP-DUb was expressed in indicated strains and localisation confirmed by Airyscan confocal microscopy. ***G)*** Histogram showing mean relative growth of *rcy1*Δ and *ist1*Δ mutants compared with wild-type cells across media containing indicated concentrations of tryptophan, n = 3 biological repeats, with error bars showing standard deviation * represents $p < 0.02$ from unpaired *t*-test. ***H)*** FM4-64 efflux measurements from wild-type, *rcy1*Δ, and *ist1*Δ cells grown to mid-log phase prior to loading with dye for 8 minutes at room temperature and cold washes. Scale bar, white denotes 5 µm and yellow denotes 0.5 µm.

As Ist1 has been implicated in polymerisation and creation of cytosolic recycling tubules[59–61], we reasoned this function could be conserved in yeast (**Figure 5A**). If yeast Ist1 polymerises to drive recycling, Vps4 is an obvious candidate AAA-ATPase for Ist1 depolymerisation. However, *vps4*Δ exhibit only a marginal defect in FM4-64[39] and a mutant of Ist1 with significantly diminished Vps4-binding[46,56] (Ist1$^{\Delta MIM}$) rescues efficient FM4-64 recycling of *ist1*Δ cells to the same extent as wild-type Ist1 (**Figure 5B**). Other mutants that affect Vps4 activity[56] also recycle FM4-64 efficiently (**Figure S5**). Furthermore, *vps4*Δ cells or wild-type cells expressing a dominant negative E233Q mutation[52] efficiently recycle Ste3-GFP-DUb (**Figure 5C**). To explore if Vps4-independent recycling relied on a distinct ATPase, we surveyed GO enrichments of recycling machinery[39] for candidates (**Figure 5D**). Apart from lipid modifying ATPases, Npl4, a non-essential adaptor of the Cdc48 ATPase was confirmed as required for recycling (**Figure 5E - 5F**) in addition to Cdc48 itself, as temperature sensitive mutants which fail to efficiently recycle Ste3-GFPDUb and FM4-64 (**Figure 5G - 5H**). This led to our speculative model that the role of Cdc48-Npl4 in recycling was mediated via Ist1, and the hypothesis that Ist1 ubiquitination would allow Cdc48 recruitment via the well-established Npl4-ubiquitin binding motif[64]. Although Ist1 is known to be turned over by the proteasome[58], it has not been formally demonstrated to be ubiquitinated, likely owning to the abundance of Lys / Arg residues (50 / 298 amino acids) that promote extensive tryptic digestion and prohibit mass-spec identification of ubiquitin modified peptides. We therefore performed a denatured ubiquitome purification[18,34,65] to reveal that ubiquitinated species of Ist1 could be observed following enrichment (**Figure 5I**). Our model would predict that ubiquitination of Ist1 is required for recycling, promoting recruitment of Cdc48 via Npl4 (**Figure 5J**). In support of this, Ist1-HA supports recycling of *ist1*Δ cells to wild-type levels, but a mutant resistant to ubiquitination (Ist1^{KR}-HA) was as defective as *ist1*Δ null cells (**Figure 5K**). Additionally, although localisation of ubiquitination defective mutants (either KR or DUb fusion) showed no significant signs of defective localisation in the presence of a wild-type Ist1, Ist1^{KR}-GFP as the sole copy accumulates in more numerous, smaller, endosomal puncta (**Figure 5L**). Most strikingly, Ist1-GFP-DUb shows very little membrane recruitment when expressed in *ist1*Δ cells. As deletion of early ESCRT subunits redistributes Ist1 to cytoplasm[47], Ist1-GFP-DUb may mimic other ESCRT-DUb fusions that inhibit endosomal recruitment[36]. In wild-type cells, Ist1-GFP-DUb localises to distinct and Vps4-mCherry marked compartments (**Figure 5M**). Minimally, these data suggest a connection between Ist1 ubiquitination and its accumulation at endosomes.

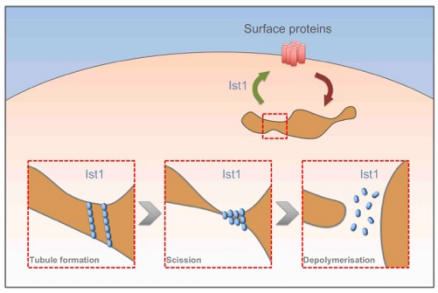

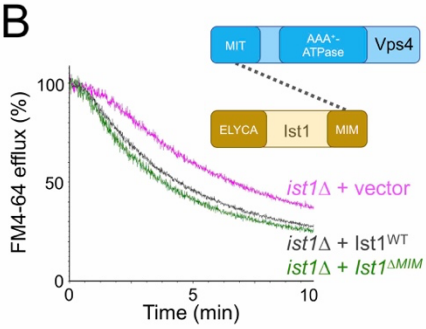

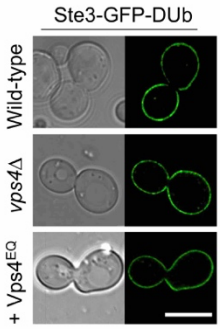

D

Selected molecular function slim terms		
GO term	**Description**	**Genes**
GO:0016787	Hydrolase activity	*CDA2, HDA1, HOS2, NEM1, PTC1, RAS2,R PD3, SIT4, YNL010W, YVH1*
GO:0003924	GTPase activity	*GPA1, GTR1, GTR2, RAS2, YPT11, YPT31, YPT32, YPT6*
GO:0019899	Enzyme binding	*DEP1, **NPL4**, STE5, VAM6*
GO:0016887	ATPase	*CDC50, DRS2, LEM3, VMA16*
GO:0032182	Ubiquitin-like binding	***NPL4***

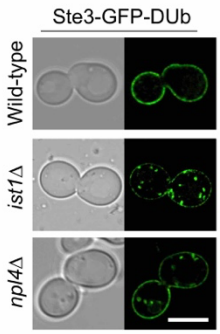

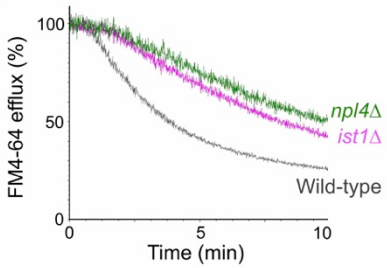

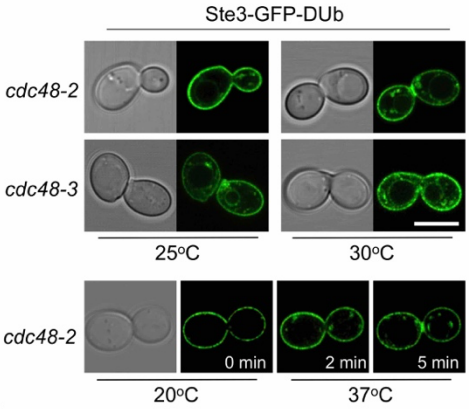

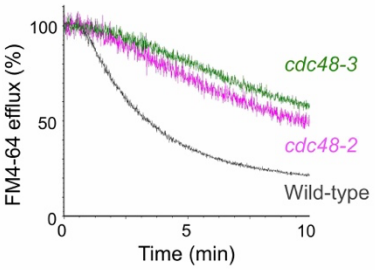

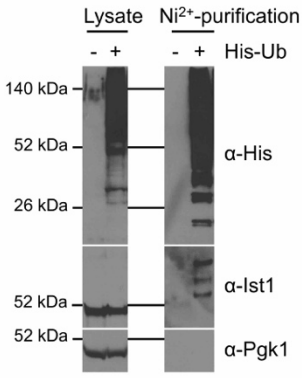

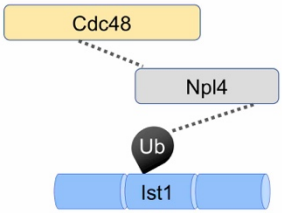

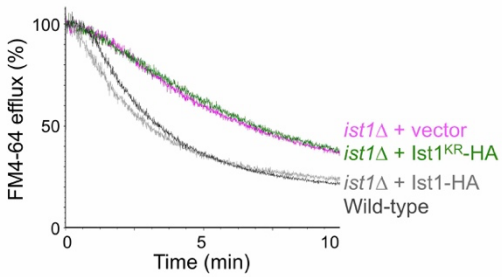

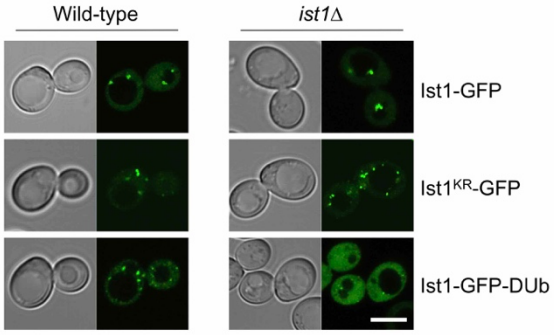

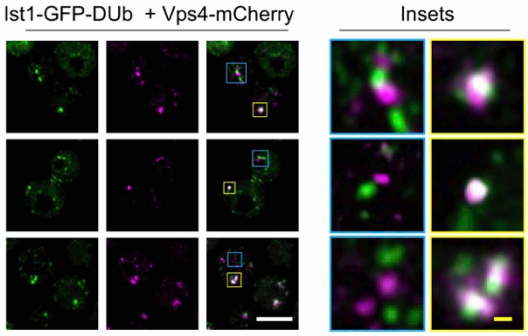

Figure 5: Ubiquitinated Ist1 and Cdc48 activity are required for surface recycling. ***A)*** Schematic representation of model for how Ist1 could drives recycling. Ist1 polymerisation / scission of endosome tubule formation. ***B)*** Efflux measurements were recorded from *ist1*Δ cells transformed with either vector control or plasmids expressing $Ist1^{WT}$ or $Ist1^{\Delta MIM}$ loaded with FM4-64 for 8 minutes at room temperature followed by ice cold washes. Schematic representation of domain interaction between Vps4 and Ist1 (above). ***C)*** Stably integrated Ste3-GFP-DUb was expressed in wild-type and *vps4*Δ cells, and also in the presence of $Vps4^{EQ}$ expressed from the *CUP1* promoter in the presence of 100 μM copper chloride before processing and Airyscan confocal microscopy. ***D)*** Table showing selected slim term annotations for recycling machinery associated with relevant enzyme activity that exhibit enrichment compared with genome-wide distribution. ***E)*** Stably integrated Ste3-GFP-DUb expressed in wild-type, *ist1*Δ, and *npl4*Δ cells imaged by Airyscan confocal microscopy. ***F)*** FM4-64 efflux measurements from wild-type, *npl4*Δ, and *ist1*Δ cells grown to mid-log phase prior to loading with dye for 8 minutes at room temperature. ***G)*** Stably integrated Ste3-GFP-DUb was expressed in strains habouring temperature sensitive alleles of *CDC48* (*cdc48-2* and *cdc48-3*), grown to mid-log phase at 25°C, and imaged by Airyscan confocal microscopy directly or following a 30-minute incubation at 30°C. ***H)*** FM4-64 efflux measurements from wild-type, *cdc48-2*, and *cdc48-3* cells grown to mid-log phase prior to loading with dye for 8 minutes at room temperature and efflux measured after 3x label free media on ice. ***I)*** Wild-type and His_6-ubiquitin expressing cells were grown to log-phase before ubiquitinated proteins were isolated from a denatured lysate (see methods). Original lysates (left) and purified samples (right) were analysed by SDS-PAGE followed by immunoblot with the indicated antibodies. ***J)*** Simplified representation of interactions (dotted lines) established between Cdc48, Npl4 and Ubiquitin. We hypothesize this enzyme module functionally connects with Ist1 via Ist1 ubiquitination. ***K)*** FM4-64 efflux measurements from wild-type cells and *ist1*Δ cells transformed with plasmids expressing $Ist1^{WT}$-HA, $Ist1^{KR}$-HA, or pRS315 vector control grown to mid-log phase prior to loading with dye for 8 minutes at room temperature. ***L)*** Wild-type (left) and *ist1*Δ (right) cells expressing GFP labelled Ist1, $Ist1^{KR}$, and Ist1 conjugated with GFP-DUb under *CUP1* promoter. Cells grown to mid-log phase in the presence of 100 μM copper chloride and processed for Airyscan confocal microscopy. ***M)*** Airyscan confocal microscopy images of wild-type cells expressing Vps4-mCherry and Ist1-GFP-DUb under *CUP1* control. Cells grown to mid-log phase in the presence of 100 μM copper chloride before processing for airyscan confocal microscopy, including enlarged insets (right). Scale bar, white denotes 5 μm and yellow denotes 0.5 μm.

DISCUSSION

Material from the PM commonly traffics through multiple compartments, for example those defined by cargo transit time, such as early- and late-endosomes. Similarly, PM cargoes also traverse compartments defined by their function, including the TGN, multivesicular bodies, and pre-vacuolar compartments. One might argue these definitions are sometimes unhelpful, as trafficking / maturation events could occur between pre-defined compartments, and trafficking time and itinerary can vary between cargoes and experimental systems / organisms, which all share this nomenclature. These issues are exacerbated by markers used to define a given compartment, which may not faithfully represent a compartment exclusively, given the dynamic nature of the endolysosomal system. In this work, we show that the retrograde / TGN recycling cargoes Snc1 / Snc2 exhibit several distinct features from the recycling of nutrient transporters Mup1 and Fur4. Snc1 / Snc2 mainly internalise to Sec7 compartments, exhibit polarised distribution in daughter cells and their trafficking is perturbed by cargo deubiquitination (**Figures 1 & 2**). Mup1/Fur4 internalise to Vps4-Ist1 compartments, localises predominantly to mother cells during cell division, and deubiquitination triggers their recycling. As ubiquitination status of nutrient transporters is controlled in response to extracellular substrate[66], we found evidence that both internalisation and recycling via Vps4-Ist1 endosomes of fluorescently tagged Mup1 could be observed in real time by modulating extracellular methionine (**Figures 3 & 4**). Given Mup1 internalises to Vps4-Ist1 endosomes in the scale of seconds to minutes, these compartments could be considered yeast early endosomes. Furthermore, our imaging and biochemical data suggest internalised Mup1 recycles back to the surface from Ist1-Vps4 compartments, allowing them to also be considered as yeast recycling endosomes. Given the large amount of data showing Vps4 is a critical regulator of MVB formation[67], and therefore also used as a late endosome / multivesicular body marker, it may be that cargo recycling / degradation fates are decided from the same compartment, or that distinct populations[11] (**Movie S6**) are functionally distinct despite sharing some of the same machinery.

Although endosomal recycling of cargo in mammalian cells is complex[68–70], our observations support the notion that recycling characteristics are evolutionarily conserved and can be elucidated using yeast. To initiate exploration in this direction, we followed up on the observation that Ist1 is required for the recycling pathway triggered by deubiquitination[39], as the mammalian orthologue of Ist1 regulates endosomal recycling in animal cells[59–61]. We demonstrate that yeast Ist1 is ubiquitinated, which is required for proper endosomal recruitment and recycling capacity (**Figures 5**). It is tempting to speculate that the role of Ist1 in yeast recycling depends on its polymerisation / depolymerisation, but further work is required to establish if this feature is conserved and how Ist1 could be co-regulated alongside other ESCRT-III subunits and other functions like MVB sorting[14,59,71]. If depolymerisation of Ist1, or indeed other factors, is required for recycling, our work suggests that Vps4 is not the primary ATPase involved. However, we do find the ATPase Cdc48 (p97 / VCP), in collaboration with the ubiquitin-binding adaptor Npl4, is required for recycling; both of which are highly conserved[72], further suggesting a fundamental membrane trafficking mechanism.

METHODS

Reagents

Supplemental tables are included to document use of plasmids (**Table S1**), yeast strains (**Table S2**), primary antibodies (**Table S3**), and statistical analysis (**Table S4**).

Cell culture

Saccharomyces cerevisiae yeast strains were cultured in synthetic complete minimal media (SC; 2% glucose, yeast nitrogen base supplemented with base / amino acid drop out mixtures for selections) or yeast extract peptone dextrose (YPD; 2% glucose, 2% peptone, 1% yeast extract). Yeast cultures were typically grown in serial dilution overnight to allow for harvesting at mid-log phase (OD_{600} ≤ 1.0) prior to experimentation, unless otherwise stated. Selection for strains harbouring KanMX cassettes were carried out in rich media containing 250 µg/ml geneticin/G418 (Formedium). The mCherry and GFP fusions of *SEC7* were generated with a methotrexate cassette selected on SC media containing 20 mM methotrexate (Alfa Aesar) and 5 mg/ml sulphanilamide before the *loxP* flanked cassette was excised by transient expression from a *TEF1-Cre* plasmid that was subsequently removed via 5-Fluoroorotic Acid media [73] Expression from the *CUP1* promoter was induced by the addition of 20 - 100 µM copper chloride. Methionine (20µg/ml) and uracil (40 µg/ml) were added to SC media to induce trafficking of Mup1 and Fur4, respectively.

Confocal microscopy

Yeast cells were harvested from early-mid log phase (OD_{600} ≤ 1.0) and prepared for imaging using Zeiss laser scanning confocal instruments (typically LSM880 equipped with an Airyscan or LSM780/LSM710) using the Plan-Apochromat 63x/1.4 objective lenses. The fluorescent proteins mCherry, photo-converted mEOS and mStrawberry were excited using the 561 nm line from a yellow DPSS laser and the emission range 570-620 nm was collected. The fluorescent proteins mGFP, GFP, mNeonGreen and pre-converted mEOS were excited using the 488nm line from an Argon laser, the emission range 495-550 nm was collected. The fluorescent protein mEOS was photo converted using 0.5% the 405nm laser with 5 iterations per conversion and 3 conversions of a defined region of interested as stated. YPD containing 0.8 µM FM4-64 was used to label vacuoles for 1-hour followed by 3x washing and 1-hour chase period in SC minimal media. For dual population imaging, cultures were grown independently to mid log phase before mixing 1:1 ratio and grown for a further 1-3 hours. 1 µg/ml DAPI was added to harvested cells for 10 minutes prior to imaging, and was excited using the 405nm line, the emission 460/50 nm was collected.

Microfluidics and time-lapse microscopy

Yeast cultures were grown to very early log phase (OD_{600} ≤ 0.2) and adhered to 35 mm glass bottom coverslip dishes (Ibidi GmbH, Germany) coated with concavalin A (Sigma-Aldrich) prior to live-cell imaging at room temperature. Concavalin A coating was prepared by adding 1 mg/ml concavalin A in water to the glass bottom coverslip for 5 minutes prior to three washing steps; prepared plates were routinely stored at 4°C. Sterile media exchanges were performed using 50mL syringes through tubing fused to the lid of the 35 mm dishes.

Image analysis

Airyscan micrographs were processed using Zen software (Zeiss) and were further modified using Fiji. For time-lapse movies, bleach correction was carried out using the inbuilt Fiji plugin and histogram-matching method [74]. Any necessary drift correction was carried out in Fiji using the plugins Hyper Stack Reg and Turbo Reg [75]. Fluorescence intensity measurements during photoconversion experiments was assessed in Zen Black and plotted in GraphPad (v9.0.2, Prism). Steady state colocalization measurements was performed using cell magic wand and morphological erosion to exclude surface signal was used to define intracellular populations that were then analysed by CoLoc2 plugin and Pearson coefficients reported. For time-lapse microscopy, Mander's overlap coefficients were measured for individual cells after normalisation for individual GFP and mCherry fluorescence using Zen Black (Zeiss).

FM4-64 recycling assay

Yeast were grown to mid-log phase in SC minimal media with corresponding selection to plasmid or YPD, 1 mL of cells (OD = 1.0) were harvested, incubated for 8 min at room temperature in 100 µL YPD containing 40 µM FM4-64 dye (*N*-(3-Triethylammoniumpropyl)-4-(6-(4-(Diethylamino) Phenyl) Hexatrienyl) Pyridinium Dibromide) dye. Labelled cells were then washed in ice cold SC media for 3 minutes on ice, 3 times. Final wash concentrated cells in 100 µL SC media in preparation for flow cytometry. Approximately 2500 cells were flowed per second at ~600 V using LSR Fortessa (BD Biosciences), over a 10 min time period the FM4-64 intensity was measured with excitation 561 nm, laser filter 710 / 50. Background autofluorescence was recorded using measurements from the 530 / 50 nm detector.

Immunoblotting

Equivalent amounts of yeast culture grown to mid log phase (OD_{600} = < 1.0) were harvested, treated with 500 µl 0.2 N NaOH for 3 minutes then resuspended in lysis buffer (8 M Urea, 10% glycerol, 5% SDS, 10% 2-Mercaptoethanol, 50mM Tris.HCl pH 6.8, 0.1% bromophenol blue). Proteins were resolved using SDS-PAGE and transferred to nitrocellulose membrane using the iBlot2 transfer system (ThermoFisher). The membrane was probed using the labelled antibodies and visualised using super signal Pico Plus (ThermoFisher) Enhanced chemiluminescence signal intensity was captured using an iBright™ Imager (ThermoFisher).

Statistical tests

Indicated statistical tests for experimental comparisons were performed using GraphPad (v9.0.2, Prism). An asterisk is used in graphs to denote statistically significant differences $p < 0.02$ or less (p values shown in **Table S4**).

Bioinformatics

Gene ontology term finder[76] was used to analyse all the results of the genetic screen for recycling machinery described in[39] with searches for specific enzyme activity shown. The physical interactome was acquired from YeastMine[77]

Tat2 recycling assay

Tryptophan auxotroph (*trp1Δ)* yeast cells were grown to mid log-phase before being spotted out across a 10-fold serial dilution and grown on plates of indicated Tryptophan concentrations. Yeast growth was normalised from a wild-type control on the same plate and used the calculate the growth difference, as previously described [78].

Ubiquitome purification

Yeast CMY158 optimised for ubiquitin purification [18,65] expressing His_6-tagged ubiquitin were grown over night and used to inoculate a 1 litre culture that was grown to mid-log phase before cells were harvested, treated with 0.2 N sodium hydroxide and brought up in denaturing lysis buffer (8 M urea, 50 mM Tris.HCl pH 8.5, 5% (w/v) glycerol, 2.5% SDS, 5 mM 2-mercaptoethanol). Lysates were diluted in lysis buffer lacking SDS and used to bind 2 ml bed of Ni^{2+}-NTA agarose for 2-hours. Beads were incubated 5 times with wash buffer (50 mM Tris.HCl pH 8.5, 5% (w/v) glycerol, 8 M urea, 5 mM 2-mercaptoethanol) containing 10 mM imidazole before elution in wash buffer at pH 4.5. Sample was then neutralised, bound to 200µl bed of Ni^{2+}-NTA agarose for a further 2 hours, before repeat washes and elutions performed in wash buffer containing 350 mM imidazole. Loading buffer was added to samples and downstream SDS-PAGE and immunoblot analysis.

ACKNOWLEDGMENTS

We would like to thank Dave Katzmann (Mayo Clinic) for Ist1 antibodies and expression plasmids, David Teis (University of Innsbruck) and Jeff Brodsky (University of Pittsburgh) for yeast strains, Rob Piper (University of Iowa) and Markus Babst (University of Utah), and Chris Stefan (LMCB, UCL) for helpful discussions. Thanks also to staff at York Bioscience Technology Facility, in particular Pete O'Toole, Jo Marrison, Karen Hogg and Graeme Park for help with imaging and extensive photoconversion optimisation. This research was supported by a Sir Henry Dale Research Fellowship from the Wellcome Trust and the Royal Society 204636/Z/16/Z (CM).

DECLARATION OF INTERESTS

The authors declare no competing interests.

REFERENCES

1. Laidlaw, K. M. E. *et al.* A glucose-starvation response governs endocytic trafficking and eisosomal retention of surface cargoes in budding yeast. *J Cell Sci* **134**, jcs257733 (2020).
2. Müller, M. *et al.* The coordinated action of the MVB pathway and autophagy ensures cell survival during starvation. *Elife* **4**, e07736 (2015).
3. MacGurn, J. A., Hsu, P.-C., Smolka, M. B. & Emr, S. D. TORC1 Regulates Endocytosis via Npr1-Mediated Phosphoinhibition of a Ubiquitin Ligase Adaptor. *Cell* **147**, 1104 1117 (2011).
4. Urbanowski, J. L. & Piper, R. C. Ubiquitin Sorts Proteins into the Intralumenal Degradative Compartment of the Late-Endosome/Vacuole. *Traffic* **2**, 622 630 (2001).
5. Katzmann, D. J., Babst, M. & Emr, S. D. Ubiquitin-Dependent Sorting into the Multivesicular Body Pathway Requires the Function of a Conserved Endosomal Protein Sorting Complex, ESCRT-I. *Cell* **106**, 145 155 (2001).
6. Shields, S. B. *et al.* ESCRT ubiquitin-binding domains function cooperatively during MVB cargo sorting. *J Cell Biology* **185**, 213 224 (2009).
7. Hanson, P. I., Roth, R., Lin, Y. & Heuser, J. E. Plasma membrane deformation by circular arrays of ESCRT-III protein filaments. *J Cell Biology* **180**, 389 402 (2008).

8. Saksena, S., Wahlman, J., Teis, D., Johnson, A. E. & Emr, S. D. Functional Reconstitution of ESCRT-III Assembly and Disassembly. *Cell* **136**, 97 109 (2009).
9. Wollert, T., Wunder, C., Lippincott-Schwartz, J. & Hurley, J. H. Membrane scission by the ESCRT-III complex. *Nature* **458**, 172 177 (2009).
10. Shestakova, A. *et al.* Assembly of the AAA ATPase Vps4 on ESCRT-III. *Mol Biol Cell* **21**, 1059 1071 (2010).
11. Adell, M. A. Y. *et al.* Recruitment dynamics of ESCRT-III and Vps4 to endosomes and implications for reverse membrane budding. *Elife* **6**, e31652 (2017).
12. Maity, S. *et al.* VPS4 triggers constriction and cleavage of ESCRT-III helical filaments. *Sci Adv* **5**, eaau7198 (2019).
13. Tang, S. *et al.* Structural basis for activation, assembly and membrane binding of ESCRT-III Snf7 filaments. *Elife* **4**, e12548 (2015).
14. Pfitzner, A.-K. *et al.* An ESCRT-III Polymerization Sequence Drives Membrane Deformation and Fission. *Cell* **182**, 1140-1155.e18 (2020).
15. Hein, C., Springael, J., Volland, C., Haguenauer-Tsapis, R. & André, B. NPI1, an essential yeast gene involved in induced degradation of Gap1 and Fur4 permeases, encodes the Rsp5 ubiquitin—protein ligase. *Mol Microbiol* **18**, 77–87 (1995).
16. Keener, J. M. & Babst, M. Quality Control and Substrate-Dependent Downregulation of the Nutrient Transporter Fur4. *Traffic* **14**, 412 427 (2013).
17. Isnard, A.-D., Thomas, D. & Surdin-Kerjan, Y. The Study of Methionine Uptake inSaccharomyces cerevisiaeReveals a New Family of Amino Acid Permeases. *J Mol Biol* **262**, 473–484 (1996).
18. MacDonald, C., Shields, S. B., Williams, C. A., Winistorfer, S. & Piper, R. C. A Cycle of Ubiquitination Regulates Adaptor Function of the Nedd4-Family Ubiquitin Ligase Rsp5. *Curr Biology Cb* (2020) doi:10.1016/j.cub.2019.11.086.
19. Sardana, R. & Emr, S. D. Membrane Protein Quality Control Mechanisms in the Endo-Lysosome System. *Trends Cell Biol* (2021) doi:10.1016/j.tcb.2020.11.011.
20. MacDonald, C. & Piper, R. C. Cell surface recycling in yeast: mechanisms and machineries. *Biochem Soc T* **44**, 474 478 (2016).
21. Day, K. J., Casler, J. C. & Glick, B. S. Budding Yeast Has a Minimal Endomembrane System. *Dev Cell* **44**, 56 72.e4 (2018).
22. Laidlaw, K. M. E. & MacDonald, C. Endosomal trafficking of yeast membrane proteins. *Biochem Soc T* **46**, 1551–1558 (2018).
23. Ma, M. & Burd, C. G. Retrograde trafficking and plasma membrane recycling pathways of the budding yeast Saccharomyces cerevisiae. *Traffic* (2019) doi:10.1111/tra.12693.
24. Protopopov, V., Govindan, B., Novick, P. & Gerst, J. E. Homologs of the synaptobrevin/VAMP family of synaptic vesicle proteins function on the late secretory pathway in S. cerevisiae. *Cell* **74**, 855–861 (1993).
25. Valdez-Taubas, J. & Pelham, H. R. B. Slow Diffusion of Proteins in the Yeast Plasma Membrane Allows Polarity to Be Maintained by Endocytic Cycling. *Curr Biol* **13**, 1636–1640 (2003).
26. Lewis, M. J., Nichols, B. J., Prescianotto-Baschong, C., Riezman, H. & Pelham, H. R. Specific retrieval of the exocytic SNARE Snc1p from early yeast endosomes. *Molecular biology of the cell* **11**, 23 38 (2000).
27. Hettema, E. H., Lewis, M. J., Black, M. W. & Pelham, H. R. B. Retromer and the sorting nexins Snx4/41/42 mediate distinct retrieval pathways from yeast endosomes. *Embo J* **22**, 548 557 (2003).
28. Ma, M., Burd, C. G. & Chi, R. J. Distinct complexes of yeast Snx4 family SNX-BARs mediate retrograde trafficking of Snc1 and Atg27. *Traffic* **18**, 134 144 (2017).
29. Galan, J.-M. *et al.* Skp1p and the F-Box Protein Rcy1p Form a Non-SCF Complex Involved in Recycling of the SNARE Snc1p in Yeast. *Mol Cell Biol* **21**, 3105 3117 (2001).
30. Hua, Z., Fatheddin, P. & Graham, T. R. An essential subfamily of Drs2p-related P-type ATPases is required for protein trafficking between Golgi complex and endosomal/vacuolar system. *Mol Biol Cell* **13**, 3162 3177 (2002).
31. Chen, S. H. *et al.* Ypt31/32 GTPases and their novel F-box effector protein Rcy1 regulate protein recycling. *Mol Biol Cell* **16**, 178 192 (2005).
32. Furuta, N., Fujimura-Kamada, K., Saito, K., Yamamoto, T. & Tanaka, K. Endocytic recycling in yeast is regulated by putative phospholipid translocases and the Ypt31p/32p-Rcy1p pathway. *Mol Biol Cell* **18**, 295 312 (2007).
33. Hanamatsu, H., Fujimura-Kamada, K., Yamamoto, T., Furuta, N. & Tanaka, K. Interaction of the phospholipid flippase Drs2p with the F-box protein Rcy1p plays an important role in early endosome to trans-Golgi network vesicle transport in yeast. *J Biochem* **155**, 51 62 (2014).
34. Xu, P. *et al.* COPI mediates recycling of an exocytic SNARE by recognition of a ubiquitin sorting signal. *Elife* **6**, e28342 (2017).
35. Stringer, D. K. & Piper, R. C. A single ubiquitin is sufficient for cargo protein entry into MVBs in the absence of ESCRT ubiquitination. *J Cell Biology* **192**, 229 242 (2011).
36. MacDonald, C., Buchkovich, N. J., Stringer, D. K., Emr, S. D. & Piper, R. C. Cargo ubiquitination is essential for multivesicular body intralumenal vesicle formation. *Embo Rep* **13**, 331 338 (2012).
37. MacDonald, C., Stringer, D. K. & Piper, R. C. Sna3 Is an Rsp5 Adaptor Protein that Relies on Ubiquitination for Its MVB Sorting. *Traffic* **13**, 586 598 (2012).

38. MacDonald, C. *et al.* A Family of Tetraspans Organizes Cargo for Sorting into Multivesicular Bodies. *Dev Cell* **33**, 328 342 (2015).
39. MacDonald, C. & Piper, R. C. Genetic dissection of early endosomal recycling highlights a TORC1-independent role for Rag GTPases. *J Cell Biol* **8**, jcb.201702177 (2017).
40. Johnson, S. S. *et al.* Regulation of yeast nutrient permease endocytosis by ATP-binding cassette transporters and a seven-transmembrane protein, RSB1. *J Biol Chem* **285**, 35792 35802 (2010).
41. Wiederkehr, A., Avaro, S., Prescianotto-Baschong, C., Haguenauer-Tsapis, R. & Riezman, H. The F-Box Protein Rcy1p Is Involved in Endocytic Membrane Traffic and Recycling Out of an Early Endosome in Saccharomyces cerevisiae. *J Cell Biology* **149**, 397–410 (2000).
42. Seaman, M. N., McCaffery, J. M. & Emr, S. D. A membrane coat complex essential for endosome-to-Golgi retrograde transport in yeast. *The Journal of cell biology* **142**, 665 681 (1998).
43. Shi, Y., Stefan, C. J., Rue, S. M., Teis, D. & Emr, S. D. Two novel WD40 domain-containing proteins, Ere1 and Ere2, function in the retromer-mediated endosomal recycling pathway. *Mol Biol Cell* **22**, 4093 4107 (2011).
44. Best, J. T., Xu, P., McGuire, J. G., Leahy, S. N. & Graham, T. R. Yeast synaptobrevin, Snc1, engages distinct routes of postendocytic recycling mediated by a sorting nexin, Rcy1-COPI, and retromer. *Mol Biol Cell* **31**, 944–962 (2020).
45. Teis, D., Saksena, S. & Emr, S. D. Ordered Assembly of the ESCRT-III Complex on Endosomes Is Required to Sequester Cargo during MVB Formation. *Dev Cell* **15**, 578 589 (2008).
46. Dimaano, C., Jones, C. B., Hanono, A., Curtiss, M. & Babst, M. Ist1 regulates Vps4 localization and assembly. *Mol Biol Cell* **19**, 465 474 (2008).
47. Rue, S. M., Mattei, S., Saksena, S. & Emr, S. D. Novel Ist1-Did2 complex functions at a late step in multivesicular body sorting. *Mol Biol Cell* **19**, 475 484 (2008).
48. Xiao, J. *et al.* Structural basis of Ist1 function and Ist1-Did2 interaction in the multivesicular body pathway and cytokinesis. *Mol Biol Cell* **20**, 3514 3524 (2009).
49. Frankel, E. B. *et al.* Ist1 regulates ESCRT-III assembly and function during multivesicular endosome biogenesis in Caenorhabditis elegans embryos. *Nat Commun* **8**, 1439 (2017).
50. Buono, R. A. *et al.* Role of SKD1 Regulators LIP5 and IST1-LIKE1 in Endosomal Sorting and Plant Development. *Plant Physiol* **171**, 251–264 (2016).
51. Babst, M., Sato, T. K., Banta, L. M. & Emr, S. D. Endosomal transport function in yeast requires a novel AAA-type ATPase, Vps4p. *Embo J* **16**, 1820 1831 (1997).
52. Babst, M., Wendland, B., Estepa, E. J. & Emr, S. D. The Vps4p AAA ATPase regulates membrane association of a Vps protein complex required for normal endosome function. *Embo J* **17**, 2982 2993 (1998).
53. Babst, M., Katzmann, D. J., Estepa-Sabal, E. J., Meerloo, T. & Emr, S. D. Escrt-III: an endosome-associated heterooligomeric protein complex required for mvb sorting. *Developmental Cell* **3**, 271 282 (2002).
54. Nickerson, D. P., West, M. & Odorizzi, G. Did2 coordinates Vps4-mediated dissociation of ESCRT-III from endosomes. *J Cell Biology* **175**, 715 720 (2006).
55. Azmi, I. *et al.* Recycling of ESCRTs by the AAA-ATPase Vps4 is regulated by a conserved VSL region in Vta1. *J Cell Biology* **172**, 705 717 (2006).
56. Tan, J., Davies, B. A., Payne, J. A., Benson, L. M. & Katzmann, D. J. Conformational Changes in the Endosomal Sorting Complex Required for the Transport III Subunit Ist1 Lead to Distinct Modes of ATPase Vps4 Regulation. *J Biol Chem* **290**, 30053 30065 (2015).
57. Han, H., Monroe, N., Sundquist, W. I., Shen, P. S. & Hill, C. P. The AAA ATPase Vps4 binds ESCRT-III substrates through a repeating array of dipeptide-binding pockets. *Elife* **6**, e31324 (2017).
58. Jones, C. B. *et al.* Regulation of Membrane Protein Degradation by Starvation-Response Pathways. *Traffic* **13**, 468 482 (2012).
59. McCullough, J. *et al.* Structure and membrane remodeling activity of ESCRT-III helical polymers. *Science* **350**, 1548 1551 (2015).
60. Allison, R. *et al.* An ESCRT-spastin interaction promotes fission of recycling tubules from the endosome. *J Cell Biology* **202**, 527 543 (2013).
61. Allison, R. *et al.* Defects in ER-endosome contacts impact lysosome function in hereditary spastic paraplegia. *J Cell Biol* **216**, 1337 1355 (2017).
62. Menant, A., Barbey, R. & Thomas, D. Substrate-mediated remodeling of methionine transport by multiple ubiquitin-dependent mechanisms in yeast cells. *Embo J* **25**, 4436–4447 (2006).
63. Lin, C. H., MacGurn, J. A., Chu, T., Stefan, C. J. & Emr, S. D. Arrestin-Related Ubiquitin-Ligase Adaptors Regulate Endocytosis and Protein Turnover at the Cell Surface. *Cell* **135**, 714 725 (2008).
64. Wang, B. *et al.* Structure and Ubiquitin Interactions of the Conserved Zinc Finger Domain of Npl4*. *J Biol Chem* **278**, 20225–20234 (2003).
65. MacDonald, C., Winistorfer, S., Pope, R. M., Wright, M. E. & Piper, R. C. Enzyme reversal to explore the function of yeast E3 ubiquitin-ligases. *Traffic* **18**, 465 484 (2017).
66. Schothorst, J. *et al.* Yeast nutrient transceptors provide novel insight in the functionality of membrane transporters. *Curr Genet* **59**, 197–206 (2013).

67. McCullough, J., Frost, A. & Sundquist, W. I. Structures, Functions, and Dynamics of ESCRT-III/Vps4 Membrane Remodeling and Fission Complexes. *Annu Rev Cell Dev Bi* **34**, 85–109 (2018).
68. Grant, B. D. & Donaldson, J. G. Pathways and mechanisms of endocytic recycling. *Nat Rev Mol Cell Bio* **10**, 597 608 (2009).
69. Goldenring, J. R. Recycling endosomes. *Curr Opin Cell Biol* **35**, 117–122 (2015).
70. O'Sullivan, M. J. & Lindsay, A. J. The Endosomal Recycling Pathway—At the Crossroads of the Cell. *Int J Mol Sci* **21**, 6074 (2020).
71. Nguyen, H. C. *et al.* Membrane constriction and thinning by sequential ESCRT-III polymerization. *Nat Struct Mol Biol* **27**, 392–399 (2020).
72. Ye, Y., Tang, W. K., Zhang, T. & Xia, D. A Mighty "Protein Extractor" of the Cell: Structure and Function of the p97/CDC48 ATPase. *Frontiers Mol Biosci* **4**, 39 (2017).
73. MacDonald, C. & Piper, R. C. Puromycin- and methotrexate-resistance cassettes and optimized Cre-recombinase expression plasmids for use in yeast. *Yeast* **32**, 423 438 (2015).
74. Miura, K. Bleach correction ImageJ plugin for compensating the photobleaching of time-lapse sequences. *F1000research* **9**, 1494 (2020).
75. Thevenaz, P., Ruttimann, U. E. & Unser, M. A pyramid approach to subpixel registration based on intensity. *Ieee T Image Process* **7**, 27–41 (1998).
76. Cherry, J. M. *et al.* Saccharomyces Genome Database: the genomics resource of budding yeast. *Nucleic Acids Res* **40**, D700–D705 (2012).
77. Balakrishnan, R. *et al.* YeastMine—an integrated data warehouse for Saccharomyces cerevisiae data as a multipurpose tool-kit. *Database* **2012**, bar062 (2012).
78. Paine, K. M., Ecclestone, G. B. & MacDonald, C. Fur4 mediated uracil-scavenging to screen for surface protein regulators. *Biorxiv* 2021.05.27.445995 (2021) doi:10.1101/2021.05.27.445995.